The fluid thermal field over a flat heated disk

Brian D. Landers[1*], Peter J. Disimile[2], Norman Toy[1]

[1] Engineering & Scientific Innovations Inc., Cincinnati, OH 45246, USA
[2] UC-FEST, Department of Aerospace Engineering, University of Cincinnati, Cincinnati, OH 45221, USA

Email: brianlanders15@gmail.com

ABSTRACT

Numerous fires in the aviation community are typically initiated and sustained when a flammable fluid leaks onto a heated surface sometimes resulting in a catastrophic event. Due to the complex fluid thermal nature of these phenomena a two-prong effort was undertaken. Within this phase of the effort the focus is to provide insight into the fluid dynamic and thermal nature of a flow field induced by a heated surface. To this end the current work discusses the temperature and velocity fields immediately above a circular flat plate 20 cm diameter and which was heated to temperatures between 150 °C and 550 °C. Both Schlieren and laser light sheet methodologies had been used to acquire data for qualitative and quantitative examination of the flow field. It has been found that the streamlines referred to as collision lines which emanate from the edge of the plate point radially inward towards the plates center. These lines connect and form cellular structures adjacent to the plates' surface. These cell-like structures appear to be reminiscent of Rayleigh Bernard type cells of either 5 or 6 sided constructions. In addition, at certain surface temperatures, pool boiling of the fluid is initiated; however, at even higher temperatures film boiling typically occurs which is thought to lead to ignition and flame propagation. The results concluded that as the distance increases from the plate the velocity of the vortical structures increases while the temperature decreases.

Keywords: Thermal Field, Flat Heated Disk, Surface Ignition, Pool Boiling, Film Boiling.

1. INTRODUCTION

The fluid dynamic and thermal state of a fluid that surrounds a heated surface is of critical importance to the hot surface ignition problem, which is of significant interest in transportation, manufacturing, and the process industries. In fact, depending on the fluid thermal state of the surrounding fluid, the probability of ignition of flammable fluids in contact with such surfaces greatly depends on the fluid structure of the vaporizing fluid. Specifically, as a flammable liquid contacts a hot surface and begins to vaporize, the potential for fuel ignition is related to the following three general criteria. Firstly, the temperature of the heated surface must be at a sufficiently high temperature to vaporize a sufficient quantity of flammable liquid fuel. Once the fuel has been vaporized, both the fuel and surrounding ambient air must reside in a region of sufficient temperature to ensure that the ignition temperature is reached once mixed. Finally, the fuel and air must reside in close proximity to ensure the intimate mixing of the two components. The level of mixing (or turbulence) must be sufficiently high to bring the vaporized fuel and air components together forming a stoichiometric fuel air mixture, one ready for ignition.

The flow field over and above a heated flat plate (Figure 1) is regarded as a buoyancy induced flow problem where a boundary layer flow is established as a result of pressure gradients induced by density gradients, which are, in turn, are induced by the temperature gradient between the heated surface and the ambient fluid, Stewartson [1]. This results in a radial flow and symmetrical collision lines wherein the surrounding air is drawn over the heated surface.
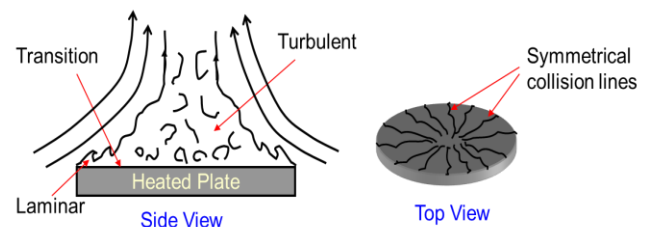
Figure 1. Hot Surface Flow Mechanism

Thermal and hydrodynamic instabilities in the boundary layer cause the flow to separate from the surface resulting in the fluid moving upwards, Pera and Gebhart [2]. Stewartson [1] also provided the first theoretical analysis of a buoyancy induced flow field on a semi-infinite heated horizontal surface placed in an expanse of fluid with Pr = 0.7. It was shown that the laminar boundary layer over such a plate is

self-similar. Rotem and Claassen [3],[4] analyzed the problem using a semi-focusing Schlieren system, whereas Pera and Gebhart [2] used an interferometric technique to investigate the extent and separation of the boundary layer for both horizontal and slightly inclined semi-infinite surfaces.

Flow over a finite plate is fundamentally different to the present circular disk surface wherein the boundary layer and corresponding flow lines originating at the leading edge of the disk would meet similar ones from all other sides of the leading edge, after which the flow turns upwards to feed into a thermal plume. The earliest visualizations of this kind of flow were provided by Croft [5], who used an interferometric technique for temperature measurements above a finite plate, and a shadow method to visualize the flow field. The observations indicated the existence of a cellular mode of convection near the surface, which was thought to be similar to the Bernard cells. Also, the observation of rising plumes above the cellular structure was thought to be due to a mushrooming effect of the cellular motion as it convects upwards. Husar and Sparrow [6] visualized the flow field over plates of various planforms, with the circular plate as a particular case, using an electrochemical technique. While they observed flow partitioning through collision lines for the boundary layer along the plate edges for each of the planforms, in the case of the circular plate, they found radially accelerating flow from the edges, which then transitioned into a billowing plume at the center. Ackroyd [7] investigated the edge flows and fluid property variations for rectangular horizontal plates and Al-Arabi and El-Riedy [8] conducted further heat transfer studies on plates of various shapes, and observed both edge and corner effects, whereas Garcia-Ybarra and Trevino [9] analyzed the thermal diffusion effects of hydrogen-air mixtures within the development of a boundary layer on a hot flat plate. Heat transfer experimental studies have also been performed circular cylindrical conduit [12], on finned tubes to determine the effect on refrigeration efficiency [13], and basic analysis on a heated cylinder [18]. Although these experiments are slightly different than the current study, they agree with the general trends of heat transfer of the current study.

Additionally, computational studies have been performed in order to try and simulate this heated plate phenomenon. For example, Mellado [10] ran a direct numerical simulation of the free convection over a smooth, heated, rectangular plate to investigate unbounded, unsteady turbulent convection. Four different boundary conditions were investigated: free-slip or no-slip walls, and constant buoyancy or constant buoyancy flux. The results show that the mean buoyancy gradient and the vertical velocity fluctuation evolve toward the corresponding power laws predicted by the similarity theory. Additionally, analytical studies have been performed on a variety of projects related such as heat channels [11], heat sinks [14], fins in a heat exchanger [15] [16], a heated rotating disk [17], and direct absorber solar collector [19].

In this present study, the flow field above a horizontal hot plate was separately visualized using both a Schlieren system and a Laser light sheet methodology, while the temperature field was mapped using high-speed thermocouples at suitable locations above and on the plate surface. Since the Schlieren image integrates the density gradients along the light path, it was used to gain a qualitative view of the overall flow structure, and was to be used extensively for examining the fuel impingement process, whereas a two-dimensional laser sheet was used to investigate the plume dynamics along a vertical central section of the plate, as well as using a horizontal laser sheet at different distances above the plate

surface to observe the vortical structures within the evolving plume.

2. EXPERIMENTAL SETUP

A flat plate of 20 cm diameter was machined from a 1.27 cm thick 316 stainless steel plate (Figure 2). The plate was electrically heated using a tightly wound 18-cm heating coil embedded within the plate assembly. This was designed to enable surface temperatures approaching 973K to be achieved. The hot plate temperature was maintained within +/- 3.5°C. A series of K-type Chrome-Alumel thermocouples were embedded through the side of the plate at various distances from the radial center, thereby enable the temperature uniformity over the surface of the plate to be monitored. Thermocouples were formed from 40 gauge wires with a bare bead measuring junction. The thermocouples used had an accuracy of +/- 2.2°C and a precision of 1°C. With the flat plate position horizontally, the temperature distribution across the plate was found to be uniform with temperature variations of less than 1% at equal radial distances from the center. Similarly, radial temperatures were measured to be 2% to 3% lower than the center at the one-half radial position, and approximately 5% lower at the perimeter of the plate. In addition to plate temperature, thermocouples were also used to record the temperature distribution normal to the plate surface using a traverse with an accuracy of (+/-) 0.001 mm. For safety purposes the plate was fitted with a stainless steel catchment gutter ensuring the containment of any unburnt fuel that flowed across the plate surface.
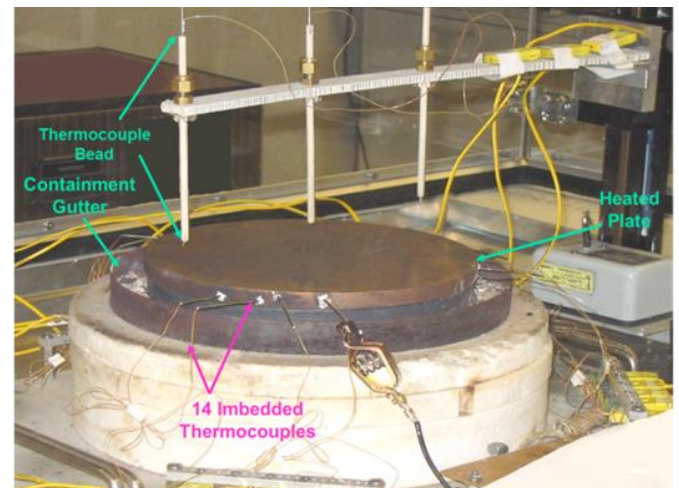
Figure 2. Hot surface set-up with thermocouples and traverse arrangement

A Schlieren system was utilized to qualitatively evaluate the flow field induced by the heated plate. Specifically the present Schlieren system was configured in a Z-type arrangement as shown in Figure 3. An illumination source 5 mm diameter was focused 2438 mm from a parabolic mirror (M1) 305 mm in diameter. Mirror M1 was used to provide a collimated light beam that was directed over the working test section (i.e., the heated plate). After passing through this test section, the light beam was directed onto a second parabolic mirror (M2) which was 349 mm diameter. This light was then focused at 2946 mm, the location of a knife-edge. The knife-edge when positioned in a vertical orientation was found to produce the best results for the current hot plate setup. The

flow field was captured with a 3-CCD Panasonic WVF250B series NTSC color video camera and displayed on a Panasonic CT-1331Y color monitor and then recorded using a Panasonic AG-7750 SVHS recorder. The video time had a resolution of 16.7 msec and the spatial resolution of the video images was 149 microns.
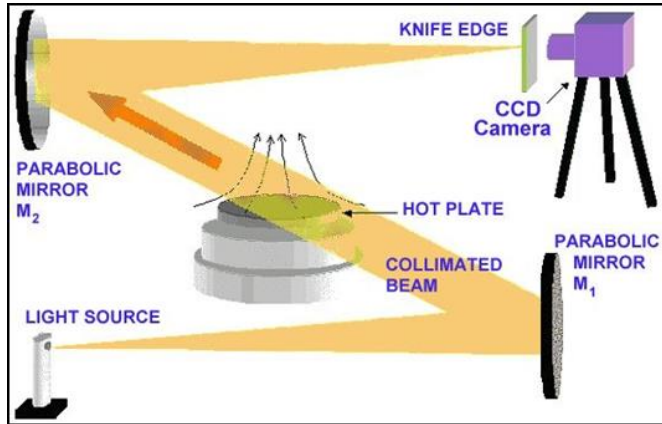

Figure 3. Z-type Schlieren System

Since previous research has shown the existence of vortical structures one method to determine the local speed of these structures is to record the images and apply image processing and structure tracking velocimetry. To provide the necessary images a laser light sheet methodology was implemented. The experimental arrangement used to generate the laser light sheet is shown in Figure 4, where an Argon-Ion Laser with a maximum output power of 4 Watts and with a wavelength range of 350-1100 nm was used. The laser sheet was developed by two methods depending on the required light intensity required. For the lower light intensity case the laser beam was passed through a cylindrical lens to form a wide light sheet (Figure 4).
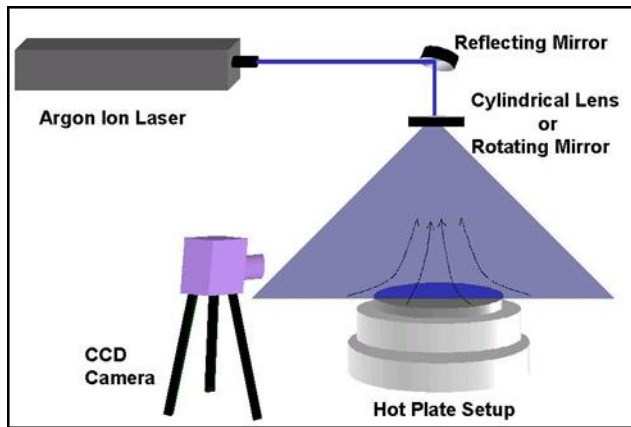

Figure 4. Laser sheet diagram

When higher light levels where required, due to the dense smoke over the hot surface the laser beam was focused onto a rotating multi-facet mirror which caused the light beam to scan the region of interest at high speed. In the current tests the mirror had 6 discrete surfaces and rotated at 2358 rpm. The flow field above the hot plate was visualized by Mie scattering of the laser light sheet that was obtained by vaporizing a petroleum product on the hot plate surface. Images of the vertical flow field were captured using the imaging equipment arranged as shown in figure 4, and for observations of the development of the plume close to the heated surface, the laser sheet was arranged horizontally.

3. RESULTS AND DISCUSSION

Images obtained from the Schlieren technique provide a qualitative overview of the thermal plume mechanism for different plate temperatures. Figure 5 shows the results of five instantaneous flow visualization images for each temperature setting of the controllers as the plate temperatures increased from 150°C to 550°C Each of the images represents instantaneous Schlieren images for each temperature setting of the controller. The actual plate surface temperatures were of the order of 100°C below the controller temperatures. The images have been enhanced using image processing software. Initially, a color-balance scheme was implemented followed by a Gaussian blur, convolution matrix analysis and masking. Then, a noise filter was applied and again a color-balance was performed.
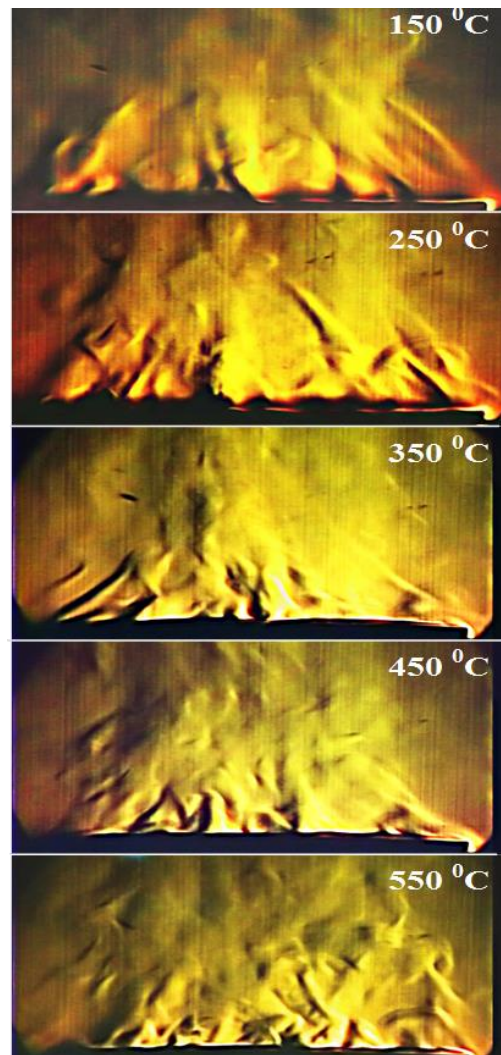

Figure 5. Schlieren images with rising plate temperature

The large-scale structures of the flow can be seen from these figures. As expected, the turbulence level in the flow increases as the surface temperature is increased. It was also observed that as the temperature of the plate is raised, the location of inception of the vortices, and their subsequent destruction could be identified. From these figures, it can be estimated that, the transition point for the breakup of the

vortices increases in height with increasing surface temperatures, as would be expected. Thus, it seems that the vortical structures, which are buoyant masses that carry a large amount of heat compared to the rest of the fluid, have greater energy and dissipate their energy at greater distance above the plate for higher surface temperatures. It must be noted that these images depict the overall flow structure since the Schlieren image represents the integrated density gradient along the light path.

Further analysis of the images presented in Figure 5 show thermal plume evolving from the edge of the hot plate. That is, when the plate temperature was set to 150 °C it can be seen that the flow is being convected radially inward towards the center of the plate before rising vertically into the plume and as the surface temperature is increased the intensity of fluid structures also increases. This mechanism suggests that there is a near and far region that governs the fluid dynamics, with a boundary layer being developed in the radial direction and extending towards the center, as distinguish by the light aqua green line in Figure 6. As these boundary layers converge upon one another (as shown in Figure 6), a transition region occurs (the near region) and the mixing process between the hot plume and entrained air evolves. This breaks down into, what appears to be, a fully developed turbulent flow in the far field region.
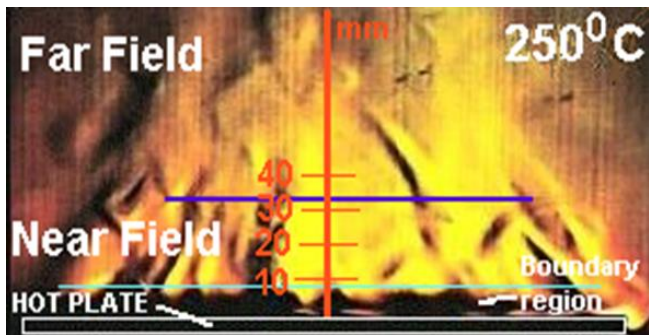
**Figure 6.** Development of the thermal plume over a hot plate at 250C

Table 1. Extent of the near field region above the hot surface

| Plate Surface Temperature (^{0}C)	Extent of the Near field Transition Zone (mm)
150	39
250	34
350	30
450	25
550	20

The results of this type of analysis for different plate temperatures between 150 °C and 550 °C has shown that as the surface temperature increases so too does the rate of boundary layer growth and this appears to increase the momentum within the near field region. This in-turn increases the turbulence within the far field at a lower elevation, which would suggest that if liquid fuel was to be dripped or leaked onto the plate at a higher temperature the likelihood of ignition would be that much greater. It is estimated that the transition zone between the near field region and the far field region is reduced from 39 mm above the surface at 150 °C, to 20 mm at 550 °C as shown in the following Table 1.

To gain some insight into the energy transfer mechanisms at work, miniature bare bead thermocouples were traversed vertically above the hot surface (Figure 7), for plate temperatures from 150°C to 550°C, in 100 degree increments. Although grouped together all plate temperatures indicate the same trend. To provide a general sense of these changes a simple linear approximation is applied and clearly indicates the existence of two thermal regions with substantially different temperature gradients. The region between the heated surface (y = 0) and the location were the slope in temperature changes significantly is referred to as the drop-off point. Figure 6 indicates for the cases tested a very sharp thermal gradient, regardless of the surface temperature setting. Even with the plate temperature set as low as 150 °C the temperature trend and drop off point appears to occur at the same approximate location for all surface temperatures tested. In all cases examined this drop off point, where the change in trend line occurs, was determined to be approximately 5 mm off the hot surface.
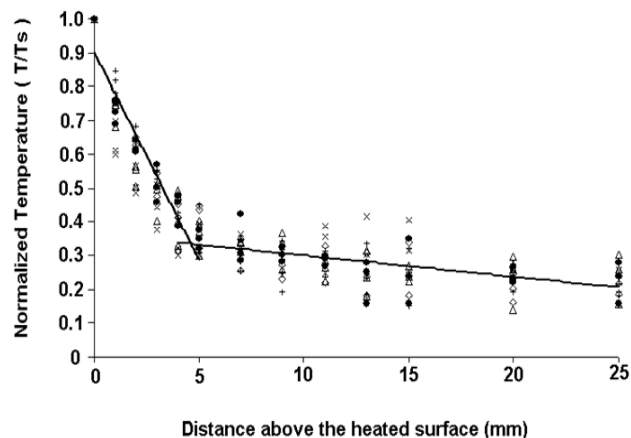

Figure 7. Temperature profiles above heated flat disks
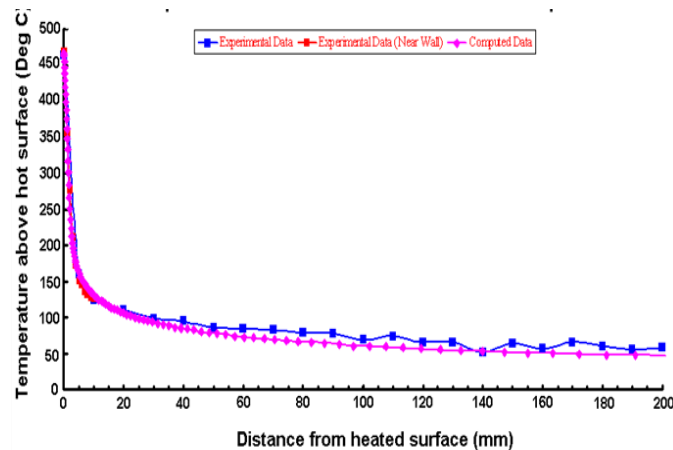
Figure 8. Experimental and CFD temperature profile above heated flat disk

To provide additional support for these steep thermal gradients and to better understand the heat transfer mechanism responsible for these gradients a detailed near wall temperature traverse was repeated as well as the initiation of a computational study. The large gradient is reminiscent of low heat transfer coefficients which are not obvious for heated surfaces under such violent natural convection conditions. Figure 8, displays the experimentally acquired temperature profile above the center of the plate when set to 450 °C, together with a computed profile using a turbulent convective model. Here it is also observed that both

the experiment and the computation shows the existence of two distinct temperature regions, one that shows a rapid decrease in temperature extending to approximately 5 mm from the surface.
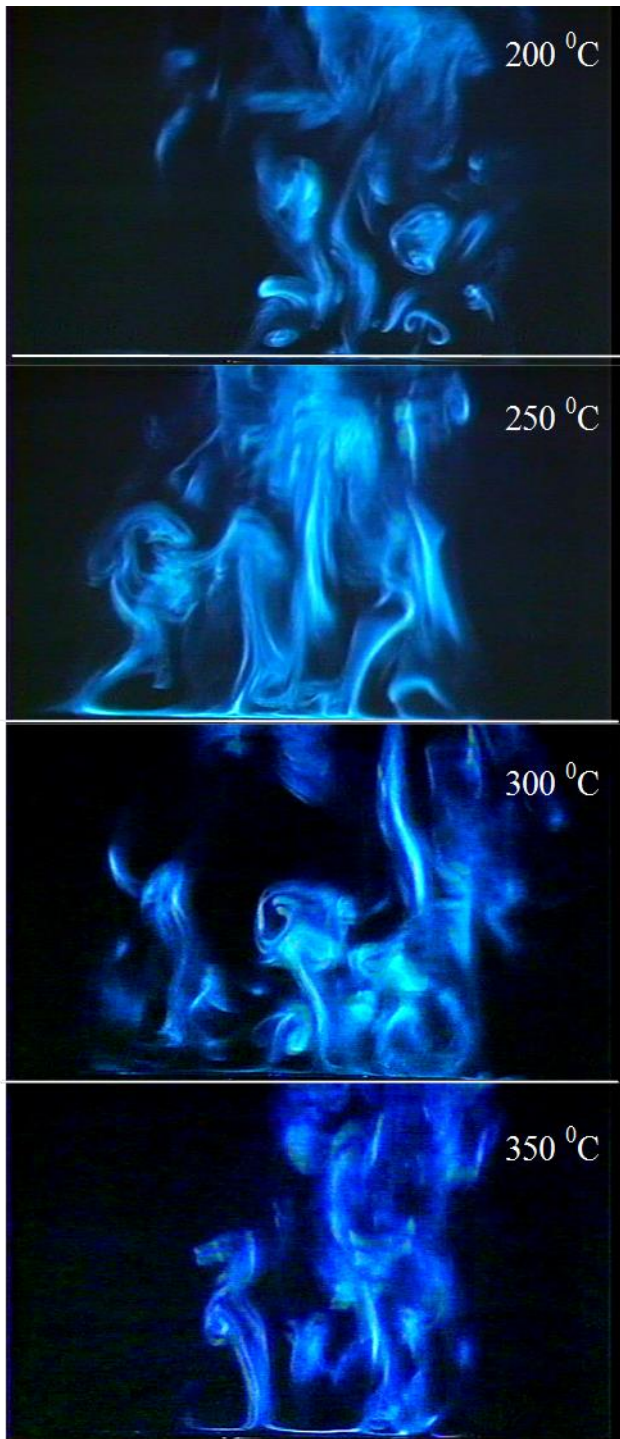

Figure 9. Visualization of the vortical structures within the thermally induced plume above the heated surface

Such profiles provide little insight into the mixing process that is evolving above the surface, and it is this mixing of the vaporizing flammable fluid and air within the high temperature region that will ultimately support and sustain ignition. Therefore to provide some further insight a second method of flow visualization was applied, laser sheet illumination. In this approach the light sheet was set perpendicular to the heated surface, and assisted in the interpretation of the fluid dynamic motions present within the

thermal plume. Images shown in Figure 9, provides a 'snapshot' of the plume as a vaporizing substance rises above the heated surface and within which vortical structures reside. Readily apparent is the stretching and convolution of these vortices as the surface temperature is increased.

There is clearly a number of different mechanisms taking place at the surface where the flow locally separates off the surface and creates well formed 'mushroom' type vortical structures before stretching and mixing with cooler ambient air that is being entrained from outside into the immediate heated zone. An estimate of the flow velocity is represented by the motion of these vortical structures as they move away from the surface can be achieved using a Lagrangian particle tracking approach. This approach enables the position of the identified vortical structures to be correlated to the frame number from which structure speed is estimated (Figure 10). This figure shows how the velocity changes with height for three different surface temperatures of 200 °C, 300 °C and 350 °C, with velocities reaching over 2 m/s at 500 mm above the surface for the 350 °C case. Although it was difficult to determine the plume velocities below about 100 mm with sufficient accuracy it is clear that the vertical velocities are small (typically < 0.5 m/s) and this is where vaporization of a leaking flammable fluid will be crucial to the ignition process.
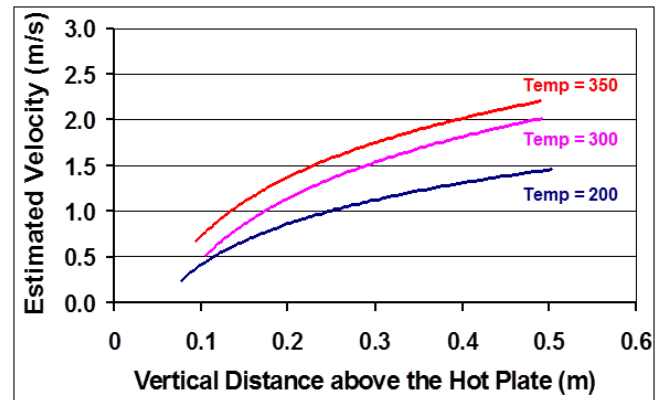

Figure 10. Velocity distribution in the plumes above the heated surface

In addition to visualizing the plume rising vertically above the surface, it was also possible to visualize the flow field in the very near region above the heated surface by rotating the laser beam parallel to the plate surface. In this case a horizontal light sheet was positioned at different distances above the heated surface and a very thin film of petroleum based product, was vaporized. The following images capture the radial movement of the boundary layer as it flows from the edge of the plate towards the center. However, the boundary layer collides and combines forming distinct cellular patterns, as are very evident in Figure 11. This figure shows two successive images "a" and "b" taken 33 msec apart (i.e., at 30 fps) and with the laser light sheet positioned 4 mm above the surface. Utilizing this frame capture rate and the position of the cell walls the velocity of the horizontal motion of the cell walls could be estimated. It should be noted that these cell boundaries are probably a projection of the rising thermals that were observed in Figure 8 and which are simultaneously moving towards the center of the plate.

How these cells form is not completely clear at the present time but they appear to be a result of a thermal instability that exists between the ambient fluid, which is being drawn into the boundary layer as it moves over the heated surface

towards the center of the plate. As shown in Figure 2 the incoming fluid tends not to penetrate into the central region (or stagnation zone) but senses the presence of this zone which is marked by the large multi-sided central cell within Figure 11. In fact this instability which causes the fluid mass to form these vortical structures is accelerated as the surface temperature is increased.
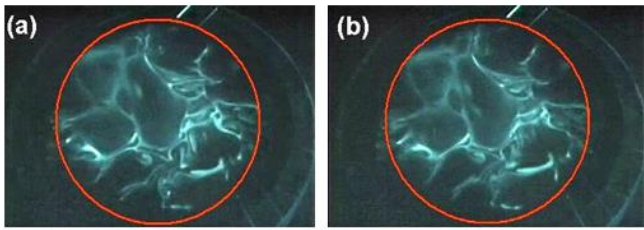
Figure 11. Two successive images of the evolving cellular pattern

Obviously, this is part of a three dimensional pattern whereby the further away from the hot surface the more rapidly the vertical component of velocity will become. However, from an analysis of the size of these cells, based on their hydraulic radius (HR = A/P), as a function of height above the surface, for different plate temperatures, it may be observed that for any given plate temperature the hydraulic radius is reduced in a linear fashion, Figure 12. Furthermore, as the plate temperature increases the HR is reduced for any given height. As height above the plate is examined it is noticed that the uncertainty in the HR also decreases as greater distances from the plate surface are approached. What is intriguing is that for plate temperatures above 250 °C the results tend to overlap at a height between 8 and 10 mm above the plate, which is synonymous with the edge of the boundary region as shown in Figure 5.
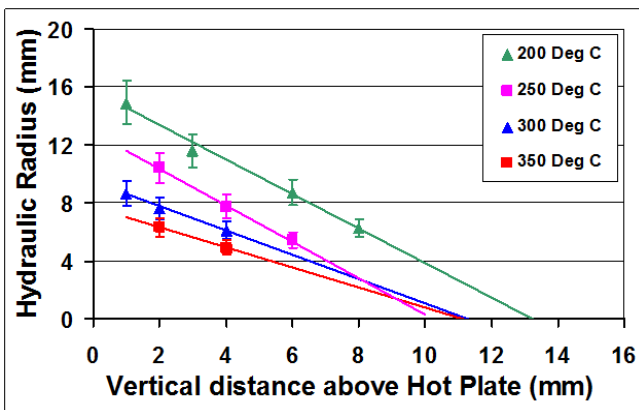

Figure 12. Hydraulic radius of the cellular patterns at different vertical locations for each temperature

Although the HR falls with increasing height for the 200 °C surface temperature case the thermal boundary layer is not as energized as those produced at the higher surface temperatures nor is the entrainment of the outside ambient conditions as vigorous. It should be noted that it was not possible to measure cellular structures below a HR of about 4 mm.

This analysis is further supported by consideration of the local horizontal velocities of the cell walls at different heights above the plate surface for each plate temperature, Figure 13, where a 3rd order polynomial has been fitted to the results to provide a general trend. These results are shown with a worse case error of about ±10% in their respective evaluations. For the cases where the surface temperature is above 250 °C there is an increase in the horizontal velocity with height up to a maximum and then it is decreases. The reason for this is that the higher above the plate the cells are, the more they will be acted upon by the rising plume and their vertical velocity component will be increasing, thereby reducing the effect of their horizontal component. Furthermore, the higher the surface temperature the lower the distance will be for the plume to start to be effective. It should be noted, that once again, temperatures < 200 °C appear not to follow this pattern and is considered to be a result of insufficient thermal energy compared to the three other cases.
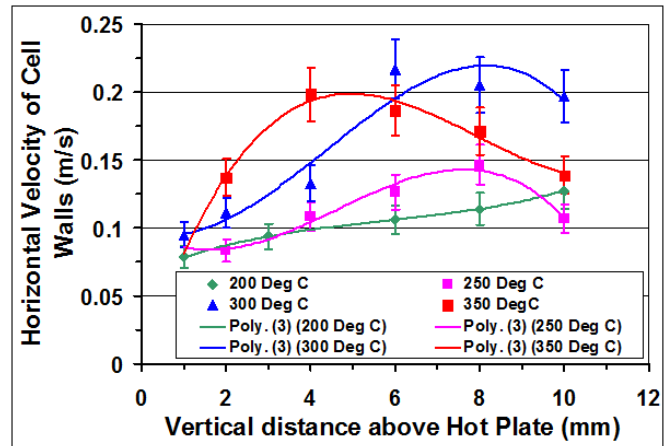
Figure 13. Horizontal velocity of the cell walls with distance above the heated surface

These horizontal velocities are much lower in magnitude than their vertical counterparts as shown in Figure 10, and were obtained with an error of about 10% in the measurement of their location. It can also be seen that the horizontal velocities do not all follow the same trend for all temperatures. All horizontal velocities, except at 250°C, rise and then began to fall as the measurements are taken further from the surface of the hot plate.

4. SUMMARY

The flow field above a heated surface has been examined using a dedicated hot surface ignition test apparatus with relatively large stable temperature range. Although the hot surface flow phenomena is complex the goal of this study provide some insight into the dominant flow phenomena and highlight the existence of the vortical structure and their dynamics as they lift off the heated surface. The ultimate goal is to couple this work with a future study on the probability ignition of a flammable fluid brought in contact with such heated surfaces.

To this end three different visualization techniques and image processing tools were applied. The visualization techniques included Schlieren, laser sheet, and scanning laser beam methodologies, to assist in providing evidence of the various fluid flow mechanisms that occur. In particular it has been demonstrated that:

(a)   As the plate temperature is increased, the size and shape of the vortical structure that makeup the flow, becomes the dominant feature.

(b) Increased surface temperature enables these mushroom vortices to grow in size, and rapidly undergo stretching and distortion,

(c) Radial collision lines are observed to emanate from the edge of the plate, travel towards the center, and appear to be attached to the apex of a forming cellular structure,

(d) The most prominent feature of the flow near the plate surface is the cell-like structure of the fluid motion that appear to be either of 5 or 6 sided in construction,

5. UNCERTAINTY

There are a few measurement uncertainties that exist in the current study: uncertainty in the thermocouples, uncertainty in temperature of the heated disk, the uncertainty in the movements of the traverse, the uncertainty of the camera resolution, and the uncertainty of the calibration technique for the image processing and structure tracking velocimetry.

The following table shows the uncertainty measurements for all applications used in the current study.

Variable	Uncertainty
Thermocouple	+/- 2.2°C
Temperature of Heated Disk	+/- 3.5°C
Traverse Movements	+/- 1 micron
Camera Resolution	+/- 149 microns
Velocity Calibration Technique	+/- 5 microns

REFERENCES

[1] Stewartson K. (1958). On the free convection from a horizontal plate, *Zeitschrift für angewandte Mathematik und Physik (ZAMP)*, Vol. 9, No. 3, pp. 276-281. DOI: 10.1007/BF02033031

[2] Pera L., Gebhart B. (1973). Natural convection boundary layer flow over horizontal and slightly inclined surfaces, *International Journal of Heat and Mass Transfer*, Vol. 16, No. 6, pp. 1131-1146. DOI: 10.1016/0017-9310(73)90126-9

[3] Rotem Z., Claassen L. (1969). Natural convection above unconfined horizontal surfaces, *Journal of Fluid mechanics*, Vol. 38, No. 1, pp. 173-192. DOI: 10.1017/S0022112069002102

[4] Rotem Z., Claassen L. (1970). Transition to quasi-cellular flow in natural convection above horizontal plates and disks, *CASI Transactions*, Vol. 3, pp. 31-34.

[5] Croft J.F. (1958). The convective regime and temperature distribution above a horizontal surface, *Quarterly Journal of the Royal Meteorological Society*, Vol. 84, No. 362, pp. 418-427. DOI: 10.1002/qj.49708436208

[6] Husar R.B., Sparrow E.M. (1968). Patterns of free convection flow adjacent to horizontal heated surfaces, *International Journal of Heat and Mass Transfer*, Vol. 11, No. 7, pp. 1206-1208. DOI: 10.1016/0017-9310(68)90036-7

[7] Ackroyd J.A.D. (1976). Laminar natural convection boundary layers on near-horizontal plates, *Proceedings of the Royal Society of London. Series A, Mathematical and Physical Sciences*, Vol. 352, No. 1669, pp. 249-274. DOI: 10.1016/0017-9310(68)90036-7

[8] Al-Arabi M., El-Reidy M.K. (1976). Natural convection heat transfer from isothermal horizontal plates of different shapes, *International Journal of Heat and Mass Transfer*, Vol. 19, No. 12, pp. 1399-1404. DOI: 10.1016/0017-9310(76)90069-7

[9] Garcia-Ybarra P.L., Trevino C. (1994). Analysis of the thermal diffusion effects on the ignition of hydrogen-air mixtures in the boundary layer of a hot flat plate, *Combustion and Flame*, Vol. 96, No. 3, pp 293-303. DOI: 10.1016/0010-2180(94)90016-7

[10] Mellado J.P. (2012). Direct numerical simulation of free convection over a heated plate, *Journal of Fluid Mechanics*, Vol. 712, pp. 418-450. DOI: 10.1017/jfm.2012.428

[11] Fakour M., Vahabzadeh A., Ganji D.D., Hatami M. (2015). Analytical study of micropolar fluid flow and heat transfer in a channel with permeable walls, *Journal of Molecular Liquids*, Vol. 204, pp. 198-204. DOI: 10.1016/j.molliq.2015.01.040

[12] Ghasemi S.E., Hatami M., Mehdizadeh Ahangar GH.R., Ganji D.D. (2014). Electrohydrodynamic flow analysis in a circular cylindrical conduit using least square method, *Journal of Electrostatics*, Vol. 72, No. 1, pp. 47-52. DOI: 10.1016/j.elstat.2013.11.005

[13] Hatami M., Mehdizadeh Ahangar GH.R., Ganji D.D., Boubaker K. (2014). Refrigeration efficiency analysis for fully wet semi-spherical porous fins, *Energy Conversion and Management*, Vol. 84, pp. 533-540. DOI: 10.1016/j.enconman.2014.05.007

[14] Pourmehran O., Rahimi-Gorji M., Hatami M., Sahebi S.A.R., Domairryd G. (2015). Numerical optimization of microchannel heat sink (MCHS) performance cooled by KKL based nanofluids in saturated porous medium, *Journal of the Taiwan Institute of Chemical Engineers*, Vol. 55, pp. 49-68. DOI: 10.1016/j.jtice.2015.04.016

[15] Ghasemi S.E., Valipour P., Hatami M., Ganji D.D. (2014). Heat transfer study on solid porous convective fins with temperature-dependent heat generation using efficient analytical method, *Journal of Central South University*, Vol. 21, No. 12, pp. 4592-4598. DOI: 10.1007/s11771-014-2465-7

[16] Hatami M., Ganji D.D., Gorji-Bandpy M. (2015). Experimental and numerical analysis of the optimized finned-tube heat exchanger for OM314 diesel exhaust exergy recovery, *Energy Conversion and Management*, Vol. 97, pp. 26-41. DOI: 10.1016/j.enconman.2015.03.032

[17] Sheikholeslami M., Hatami M., Ganji D.D. (2015). Numerical investigation of nanofluid spraying on an inclined rotating disk for cooling process, *Journal of Molecular Liquids*, Vol. 211, pp. 577-583. DOI: 10.1016/j.molliq.2015.07.006

[18] Hatami M. (2017). Nanoparticles migration around the heated cylinder during the RSM optimization of a wavy-wall enclosure, *Advanced Powder Technology*, Vol. 28, No. 3, pp. 890-899. DOI: 10.1016/j.apt.2016.12.015

[19] Hatami M., Jing D. (2017). Optimization of wavy direct absorber solar collector (WDASC) using A1$_2$O$_3$-water nanofluid and RSM analysis, *Applied Thermal Engineering*, Vol. 121, pp. 1040-1050. DOI: 10.1016/j.applthermaleng.2017.04.137